Biochemical and Biophysical Research Communications 442 (2013) 85–91

Contents lists available at ScienceDirect

Biochemical and Biophysical Research Communications

journal homepage: www.elsevier.com/locate/ybbrc

Qualitative computational bioanalytics: Assembly of viral channel-forming peptides around mono and divalent ions

Li-Hua Li, Hao-Jen Hsu [1], Wolfgang B. Fischer *

Institute of Biophotonics, School of Biomedical Science and Engineering, Biophotonics & Molecular Imaging Research Center (BMIRC), National Yang-Ming University, Taipei 112, Taiwan

ARTICLE INFO

Article history:
Received 24 August 2013
Available online 12 November 2013

Keywords:
Membrane protein
Assembly
Vpu protein
HIV-1
Molecular dynamics simulations
Docking approach

ABSTRACT

A fine-grained docking protocol was used to generate a bundle-like structure of the bitopic membrane protein Vpu from HIV-1. Vpu is a type I membrane protein with 81 amino acids. It is proposed that Vpu forms ion- and substrate-conducting bundles, which are located at the plasma membrane in the infected cell. The Vpu_{1-32} peptide that includes the transmembrane domain (TMD) is assembled into homo-pentameric bundles around prepositioned Na, K, Ca or Cl ions. For bundles with the lowest energy, the TMDs generate a hydrophobic pore. Bundles in which Ser-24 faces the pore have higher energy. The tilt of the helices in the lowest energy bundles is larger than bundles with serines facing the pore. Left-handed bundles are lowest in energy where the ions are located at the serines.

1. Introduction

Computation is an essential tool that supports various applications, such as the drug discovery process and material sciences. It is also an essential part of the available range of analytical tools [1]: e.g. it has been suggested by computational methods that additional potassium ions must be included in an ion channel structure [2]; independent from this suggestion, potassium ions have been observed in experiments [3]. This underlines the importance of applying computational methods to structure prediction. Computational methods are indispensable for deciphering patterns of protein–protein interaction, especially for transmembrane proteins [4]. In this study, a computational bioanalytical approach is applied to investigate the architecture of bundles formed by the channel-forming membrane protein Vpu from human immunodeficiency virus type 1 (HIV-1) (reviewed in [5]) in the presence of mono and divalent ions.

Vpu is a type I integral membrane protein with 81 amino acids [6,7]. It is expressed during the late stage of the infectivity cycle and enhances viral release [6,8]. This activity is attributed to the interaction between Vpu and the host factor CD317/BST-2/tetherin [9,10]. When Vpu and BST-2 interact, BST-2 is susceptible to ubiquitin-dependent down-regulation (reviewed in [11,12]). The Vpu TMD is the interaction site for BST-2 [9,10]. Before the Vpu and BST-2 interaction was discovered, viral release enhancement was solely correlated with the Vpu capacity for channel formation at the plasma membrane [13,14]. Vpu and its TMD has been reconstituted into an artificial lipid bilayer, which renderes the lipid membrane permeable to physiologically relevant ions [14–16] and small molecules [17]. The channel is also active when Vpu was expressed in *Xenopus* oocytes [14] or 293T cells [18], which is measured using a whole-cell recording experiment. However, this function has not been verified within the life cycle of the virus.

Structurally, Vpu has been reasonably well-explored by a series of spectroscopic measurements and computer simulations (reviewed in [5]). Emphasising the latter, simulations of assembled Vpu bundle TMDs have been performed primarily for a pentameric bundle [19–22]. The only hydrophilic residue, Ser-24, faces the bundle lumen in these assemblies. Only one study suggests that Trp-23 points towards the lumen [23]. Tetrameric and pentameric bundles were modelled using NMR spectroscopic data [24]. In these bundles, residues Trp-23 and Ser-24 did not face the inside of the bundles, but the hydrophobic residues form a 'hydrophobic' pore.

Results from a fine-grained docking approach with molecular dynamics simulations show that the lowest energy structures for the trimeric, tetrameric and pentameric Vpu bundles comprise the hydrophobic residues inside the lumen [25]. Structures with the serines facing the pore and forming a bundle with a 'hydrophilic' pore have high energy. These computational assembly experiments are performed without ions.

As mentioned above, investigations on KcsA have sparked the idea that the Vpu bundle should be assembled in the presence of

* Corresponding author. Address: Institute of Biophotonics, School of Biomedical Science and Engineering, National Yang-Ming University, 155, Li-Non St., Sec. 2, Taipei 112, Taiwan. Fax: +886 2 28235460.
E-mail address: wfischer@ym.edu.tw (W.B. Fischer).
[1] Current address: Department of Life Science, Tzu Chi University, Hualien 970, Taiwan.

0006-291X/$ - see front matter © 2013 Elsevier Inc. All rights reserved.
http://dx.doi.org/10.1016/j.bbrc.2013.11.017

ions. In such a protocol, the serines are expected to face the pore lumen in the lowest energy structures.

Calculations are performed for Vpu and the pore-lining M2 structural motif of proton-activated pentameric ligand-gated ion channel from *Gloebacter violaceus* (GLIC) representing an open channel [26]. Herein, helices, including the Vpu TMD, are assembled in the presence of ions using an established fine-grained docking approach [27].

2. Materials and methods

Ideal helices ($\phi = -65°$, $\psi = -39°$) in the Vpu N-terminus (Vpu HV1H2), including the TMD, were generated using the program MOE2008.10 (Molecular Operation Environment, www.chemcomp.com).

Vpu_{1-32}: MQPIPIVAIV[10] ALVVAIIIAI[20] VVWSIVIIEY[30] RK

The coordinates for the following GLIC sequence [26] are from the PDB data bank entry 3EHZ and were used without further modification:

M2: SY[220] EANVTLVVST[230] LIAHIAFNIL[240] VETN.

Both ends were modelled as uncharged groups.

2.1. MD simulations

Details on molecular dynamics (MD) simulation preparation and performance for Vpu_{1-32} have been reported elsewhere [25] and are briefly outlined herein.

Vpu_{1-32}, which is uncharged at both ends, was embedded into an equilibrated patch of a POPC lipid bilayer (POPC: 16:0–18:1 diester PC, 1-palmitoyl-2-oleoyl-*sn*-glycero-3-phosphocholine) with 128 lipids using the MOE software package. The lipids were manually removed to avoid overlapping with the peptide. The patches comprised 122 lipids (6344 atoms). The protein/lipid system was hydrated with 3655 water molecules. The pentameric ion containing bundles of Vpu_{1-32} were embedded in a respective lipid patch of 258 lipids (originally 288 lipids) and 8748 water molecules.

The MD simulations were performed using GROMACS 4.0.5 with the Gromos96 (ffG45a3) force field. The peptides, lipids, and water molecules were separately coupled to a Berendsen thermostat at 310 K with a 0.1 ps coupling time. Compressibility was set to 4.5e-5 bar^{-1}. The monomers were simulated with a semi-isotropic pressure coupling scheme. The long-range electrostatics was calculated using the particle-mesh Ewald (PME) algorithm with grid dimensions at 0.12 nm and the interpolation order 4. Lennard–Jones and short-range Coulomb interactions were cut-off at 1.4 and 0.9 nm, respectively. Water molecules were represented using the SPC model. The protein/lipid/water system was energy-minimised followed by 1.9 ns of equilibration MD simulation. The equilibration MD simulation began with a temperature increase in the system from 100 to 200 K and to 310 K. During these simulations, the peptide was restrained. At 310 K, the peptide restraints were gradually released in three steps (k = 1000 kJ mol^{-1} nm^{-2}, k = 500 kJ mol^{-1} - nm^{-2}, k = 250 kJ mol^{-1} nm^{-2}) running each step for 1.5 ns. During a 50 ns MD simulation the ions were restraint at their position at all stages during the simulation protocol.

2.2. Assembly

An average structure for the helices' backbone residues was calculated, as reported earlier [27]. Rotational and translational movements in the helices were cancelled out by fitting each consecutive helix structure to the first structure. The structures from the last 10 ns of simulation were averaged using the program g_covar from the GROMACS-4.0.7 package.

The monomers were assembled (see also [25,27]) using a program based on the scripting 'scientific vector language' (SVL) of the MOE suit. For energy calculations, the AMBER 94 force field was used with the dielectric constant at $\varepsilon = 2$. The helices were copied, positioned around a central axis (C5 symmetry), and aligned. Each ion, K^+, Na^+, Cl^- and Ca^{2+}, was placed along the central axis at various positions. Approximately 350,000 conformers were generated by sampling interhelical distances between 10 and 15 Å then screening the tilt between ±36° and the rotational angle. Each structure was minimised.

The solvent accessible surface (SAS) was calculated using the program g_SAS of the gromacs suit.

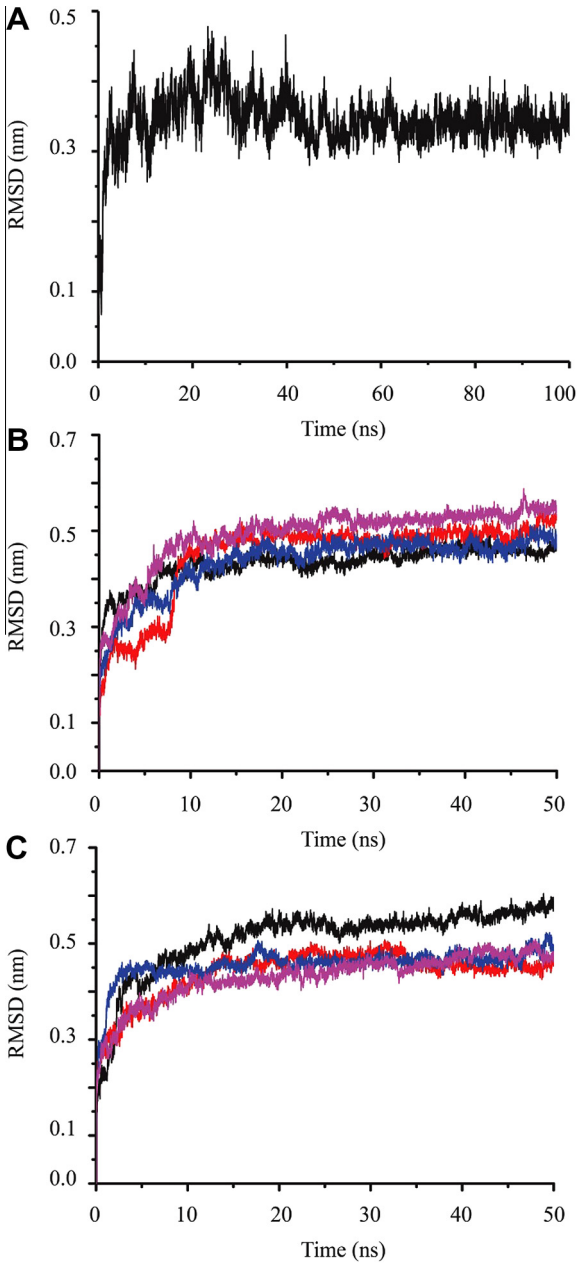

Fig. 1. RMSD values based on the Cα atoms of Vpu_{1-32} (A), the lowest-energy bundles (B) and serines-facing-pore bundles (C) of Vpu_{1-32} in the presence of restrained ions. Traces show the values for bundles with Na^+ in pink, K^+ in blue, Cl^- in red and Ca^{2+} in black. (For interpretation of color in this Figure, the reader is referred to the web version of this article.)

The simulations were prepared on a DELL T7500 workstation and submitted to the National Center for High Performance Computing (NCHC), Hsinchu, TW using 8 parallel cpus for the production run.

Plots and pictures were generated using VMD-1.8.7 and Pymol.

3. Results

A single TMD from Vpu_{1-32} is generated and embedded into a hydrated lipid bilayer composed of POPC. The RMSD values level off after a moderate rise within the first 10 ns (Fig. 1A). Further characterisation of the peptide after a 100 ns MD simulation is described elsewhere [25].

3.1. Docking approach

Each electrophysiological relevant ions, Na^+, K^+, Cl^- and Ca^{2+}, are individually placed at three positions along a central axis. The distance between the positions is 10 Å. Five copies of Vpu_{1-32} are then assembled around the ions. The ions are positioned such that they were located on the C-terminal side (assembly protocol I (P-I), see Fig. 2), the centre (P-II), and the N terminal side of the bundle (P-III). In an additional configuration, each ion is simultaneously placed at each site (P-IV).

The lowest-energy bundles using P-I with Na^+, Ca^{2+} and Cl^- show that the rim of alanines (Ala-8, -11, -15, -19) faces the pore lumen (Fig. 2A,C and D). K^+ is the only ion that induces an assembly with the serines facing the interhelical space, and the tryptophans point into the pore (Fig. 2B). The distances between the helices and pore axis are small for the bundles with Ca^{2+} (9.2 Å) and Cl^- (9.6 Å); they are large for the bundles with Na^+ (11.6 Å) and K^+ (12.2 Å) (Table 1). The bundles are left-handed except for the bundle assembled around Ca^{2+}. The potential energies for the bundles decrease with the following order: −2129 kcal/mol (Ca^{2+}) > −2257 kcal/mol (Na^+) > −2301 kcal/mol (Cl^-) > −2360 kcal/mol (K^+) (Table 1).

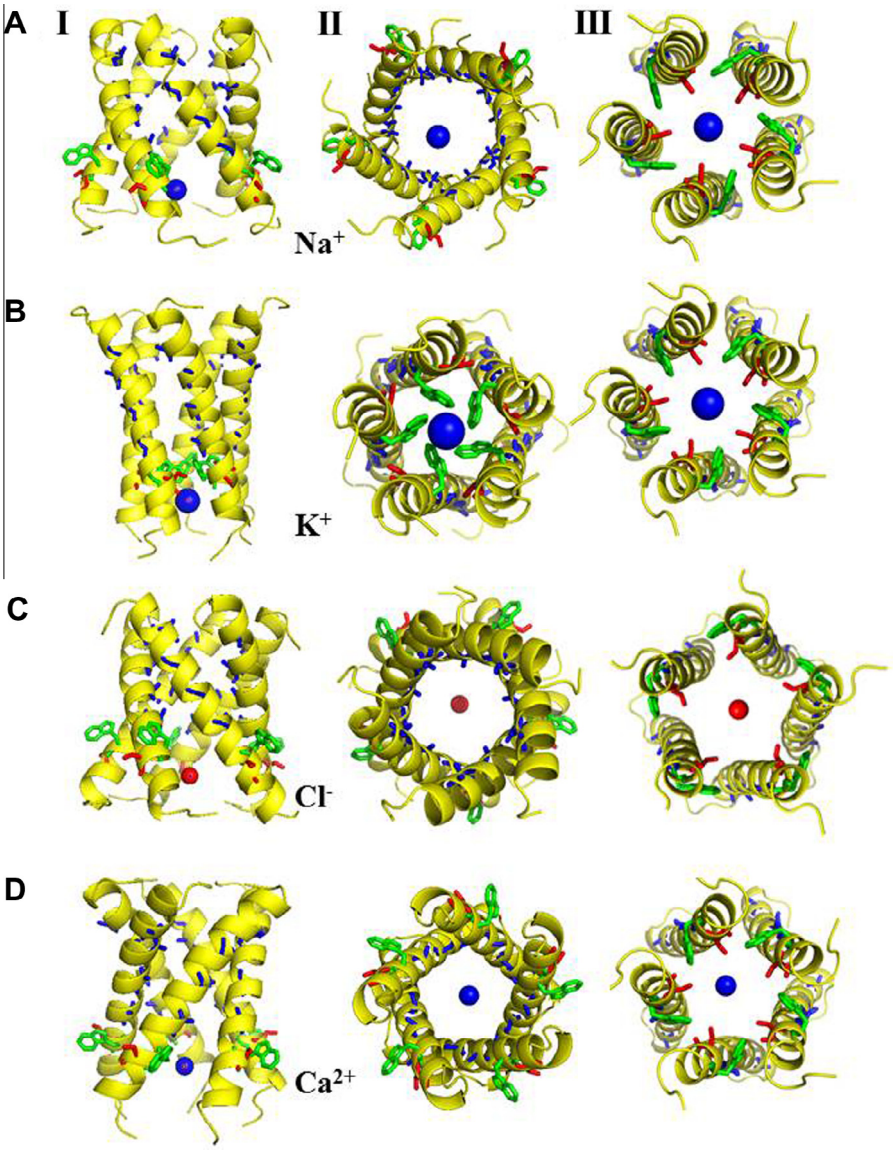

Fig. 2. Representative pentameric assemblies for Vpu_{1-32} using P-I. The bundles are shown with Na^+ (A), K^+ (B), Cl^- (C) and Ca^{2+} (D). From left to right: a side view (I) and top view from the C to N terminal mouth (II) of the lowest-energy structures and the lowest-energy structure with the serines facing the pore (III). The helix backbone is shown in yellow, as well as alanines (blue), serine (red) and tryptophan residues (green). Cations and Cl^- are shown using blue and red spheres, respectively. (For interpretation of color in this Figure, the reader is referred to the web version of this article.)

Table 1
Distance, tilt and rotational angles, as well as the assembly interaction energies for the pentameric bundles using various assembly protocols (APs). The APs can be discriminated by the ion positions at the C terminal side (P-I), at the centre (P-II) and towards the N terminal side (P-III). A protocol wherein the ions are placed at each site was referenced as P-IV. For each protocol, the upper line shows data for the lowest-energy structure (low), and the second line describes the lowest-energy structure wherein the serines face the pore (ser).

Ion and assembly protocol (AP)	Dist [Å]	Tilt [°]	Rot [°]	E [kcal/mol]	ΔE [kcal/mol] [low – ser]
Na^+					
I	11.6	34	346	−2257	147
	12.4	10	164	−2110	
II	11.8	30	334	−2249	222
	11.4	16	166	−2027	
III	11.8	28	330	−2267	175
	11.4	18	172	−2092	
IV	9.6	−34	308	−2075	80
	13	20	170	−1995	
K^+					
I	12.2	16	126	−2360	321
	13	−12	182	−2039	
II	9.2	36	348	−2308	231
	12.8	10	164	−2077	
III	9.2	36	348	−2273	228
	12.8	10	164	−2045	
IV	12.6	14	124	−2293	204
	13	−12	182	−2089	
Cl^-					
I	9.6	36	250	−2301	306
	12.8	−12	182	−1995	
II	12.6	12	122	−2293	304
	12.6	8	162	−1989	
III	11.4	36	30	−1880	215
	12	−6	222	−1665	
IV	10	34	354	−2294	355
	13	8	202	−1939	
Ca^{2+}					
I	9.2	−34	308	−2129	199
	13	20	170	−1931	
II	11.2	34	358	−2290	190
	13	14	164	−2100	
III	12.4	16	124	−2099	248
	13	12	164	−1851	
IV	13	−8	106	−2428	83
	13	10	164	−2345	

The serines-facing-pore bundles derived using P-I (Fig. 2, III), have a higher energy than the lowest-energy bundles by, for example, 147 kcal/mol (Na^+), 321 kcal/mol (K^+), 306 kcal/mol (Cl^-) and 199 kcal/mol (Ca^{2+}) (Table 1). The distance to the central axis of the bundles is larger than the distance for the lowest-energy bundles (Table 1). Except for the bundle with Na^+, the handedness of these bundles is reversed compared with the lowest-energy bundles (Table 1) composed of K^+, Cl^- (both right-handed with a −12° tilt), and Ca^{2+} (left-handed, tilt 20°).

Left-handed lowest-energy bundles are generated, except for P-IV with Ca^{2+} (right-handed, −8° tilt) and Na^+ (−34° tilt) (Table 1) for P-II through P-IV. The hydrophobic side faces the central axis in most bundles. The bundles with K^+ using P-IV, Cl^- using P-II as well as Ca^{2+} using P-III and P-IV have the serines in an interhelical location and tryptophans facing the pore. The energies for the serines-facing-pore bundles are approximately 100–300 kcal/mol (Table 1) higher than the energies for the lowest-energy bundles. In most cases, left-handedness is preserved except while using P-IV. For Ca^{2+}, the short minimisation applied in the protocol moves the ion in P-III towards the bundle centre.

The lowest-energy bundles in each assembly commonly adopt larger tilt angles, either positive or negative, compared with the serine-facing-pore bundles (Table 1). There is only one exception for the bundles with Ca^{2+} assembled using P-IV. The TMDs in the lowest-energy bundles adopt a −8° tilt, whereas they adopt a +10° tilt in the serines-facing-pore bundle.

The data herein show that the hydrophobic side of the helical TMDs faces the pore lumen. In such a conformation, serines and tryptophans are turned towards the side of the lipid bilayer. Certain lowest-energy bundles wherein the serines point 'inside' and towards the interhelical face facilitate tryptophan obstruction of the pore. Most bundles are left-handed. The tryptophans are located at the interhelical face in the serines-facing-pore bundles.

The five helical transmembrane M2 segments of GLIC (3EHZ) (Fig. 3A) are assembled to evaluate the protocol. Assembly without ions generates a pentameric bundle (Fig. 3B), which is similar to the original assembly. The bundle adopts a left-handed structure (tilt: 12°) (Table 2), and the helices are slightly rotated outwards. Thus, Ser-229, Thr-225 and Glu-242 are within the channel lumen, and the first two residues face the helix–helix interface (Fig. 3B). The amino acid orientations are maintained for each assembly protocol. Right-handed bundles are generated (around −10°) with 10–11 Å interhelical distances and −3000 to −3500 kcal/mol energies (Table 2) for most models. The bundles with Na ions produce the lowest RMSD values relative to the crystal structure compared with values from bundles composed of other ions (Table 2) using the same assembly protocol (Fig. 3C).

3.2. Short MD simulations with restraint ions

All structures which have been generated with P-I are used in a 50 ns MD simulation (Fig. 4). The ions are restraint during the simulations. The RMSD values of the lowest-energy bundles with sodium and potassium ions (Fig. 1B) as well as all of the M2 segments of GLIC (data not shown) level off within the first 10 ns. Calculated lipid thickness (values between 33.1 and 35.7 Å) and area per lipid (values between 56.7 and 64.3 $Å^2$) are within expected ranges found for POPC (Suppl. Table 1) [28]. The RMSD values of the serines-facing-pore bundles rise to a second plateau after the initial rise (Fig. 1C). Visible inspection of the bundles reveals that there is a tendency of both bundle types, lowest-energy and serines-facing-pore bundles, to turn into an oval shape by 'ejecting' one of the TMD from the bundle formation (Fig. 4). Especially the serines-facing-pore bundles arrange themselves around the ions into a tetrameric bundle. Analysis of the averaged tilt angles (Table 3) reveals that values are similar to those calculated from the assembly protocol (Tables 1 and 2). The tilts of the helices in the bundles with K^+ and Ca^{2+} adopt similar values for both bundle types. The averaged kink of the helices in all the bundles found to be in the range of 162–167°.

The SAS area of both bundle types with the ions in their centre decreases (Table 3). The largest change is found for the lowest-energy bundle with Na^+ (16%), the smallest change is found for the lowest-energy bundle with K^+ (2.1%). The sequence is reversed for the values of the serine-facing-pore bundles (4.7% for Na^+; 12.1% for K^+). There is almost no difference for the SAS values of the different bundle types for Cl^- (6.8/8.4%) and Ca^{2+} (10.4/10.6%). Based on the lowest % change, K^+ and Ca^{2+} change the serines-facing-pore bundles more than Na^+ and Cl^-. This is due to the larger size of K^+ and ion strength of Ca^{2+} as compared to Na^+ and Cl^-.

4. Discussion

An ion-conducting channel likely comprises hydrophilic residues that line the walls of the ion passageway to ease ion permeation through the protein. The primary sequence for Vpu contains a single serine, Ser-24, and it is hypothesised that this particular

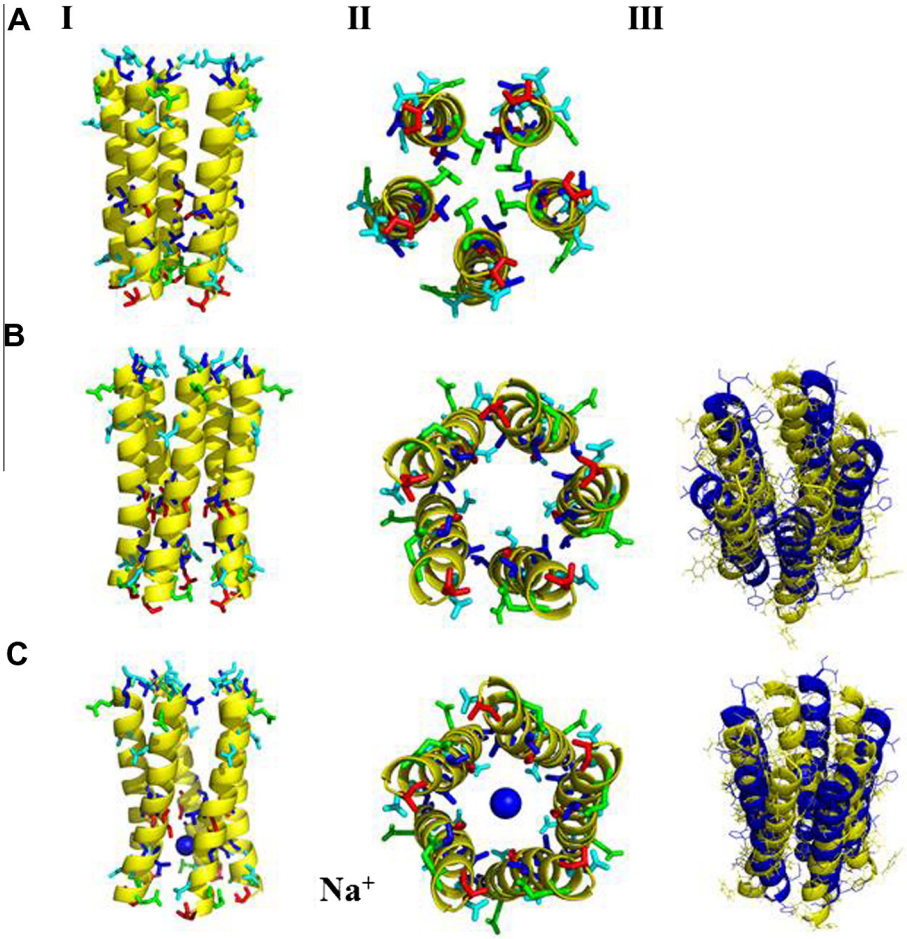

Fig. 3. The representative pentameric assemblies for the M2 domain in GLIC (3EHZ) [26]. Shown are the original structure (A), the assembled structure without ions in the centre (B) and with Na^+ placed in accordance with P-I (C). The figure shows (from left to right) a side view (I) and top view from the cytoplasmic side (II) of the lowest-energy structures (B and C) as well as (III) overlaid structures from (B) and (C) both in yellow with (A) in blue. Threonine residues (blue), serine (red) glutamate (green) and asparagine (cyan) are shown. Na^+ is represented by a blue sphere. (For interpretation of color in this Figure, the reader is referred to the web version of this article.)

Table 2
Distance, tilt and rotational angles as well as the assembly interaction energies for the M2 helices from GLIC [26] in pentameric bundles using various assembly protocols (APs).

Ion and assembly protocol (AP)	Dist [Å]	Tilt [°]	Rot [°]	*E* [kcal/mol]	RMSD [nm]
No ion	10.3	12	326	−3478	13.6
Na^+					
I	10.4	−16	326	−3433	13.8
II	10.6	−12	322	−3502	13.4
III	9.4	−12	334	−3474	13.8
IV	12.2	4	318	−2643	13.5
K^+					
I	10.6	2	6	−3314	14.2
II	10.6	−14	324	−3411	13.8
III	10.6	−14	324	−3363	13.8
IV	10.8	26	300	−3296	14.6
Cl^-					
I	10.6	−12	326	−3275	13.8
II	10.8	−16	328	−3228	14.1
III	10.8	−14	324	−3270	14.0
IV	10.8	−14	324	−3260	13.9
Ca^{2+}					
I	10.6	2	6	−3427	14.2
II	10.6	−12	326	−3442	13.8
III	10.6	−14	324	−3390	13.9
IV	13	−8	106	−2428	13.5
	13	10	164	−2345	

amino acid faces the bundle pore. Computational fine-grained assembly protocols do not produce such a Vpu bundle [25,27]. Therefore, assembly is performed in the presence of ions to 'force' the serines to face the pore lumen in this study.

4.1. Evaluation of the putative bundle architectures

In the presence of ions, hydrophobic pores, which are the lowest-energy bundles, are the most likely to be generated. In these bundles, the tryptophans point towards the lipid phase. Tryptophans typically anchor membrane proteins within a lipid bilayer by interacting with carbonyl groups on the acetylated glycerol of lipid molecules *via* the indole ring.

Likely, the tryptophans point into the pore, as has been observed under certain conditions, because the side chain favours the ion positive charges.

It can also be suggested that serines and tryptophans face the pore lumen in the presence of ions, and the serines interact with neighbouring helices. In such a configuration, only a slight rotation by the serines into the lumen would 'open' the channel. At the same time, the bulky tryptophans would move towards the helix–helix interface.

Whenever serines mantle the pore, the bundles are primarily straight (for assembly without ions, see also Table 2 published previously [25]). In such a straight position, the tryptophans are

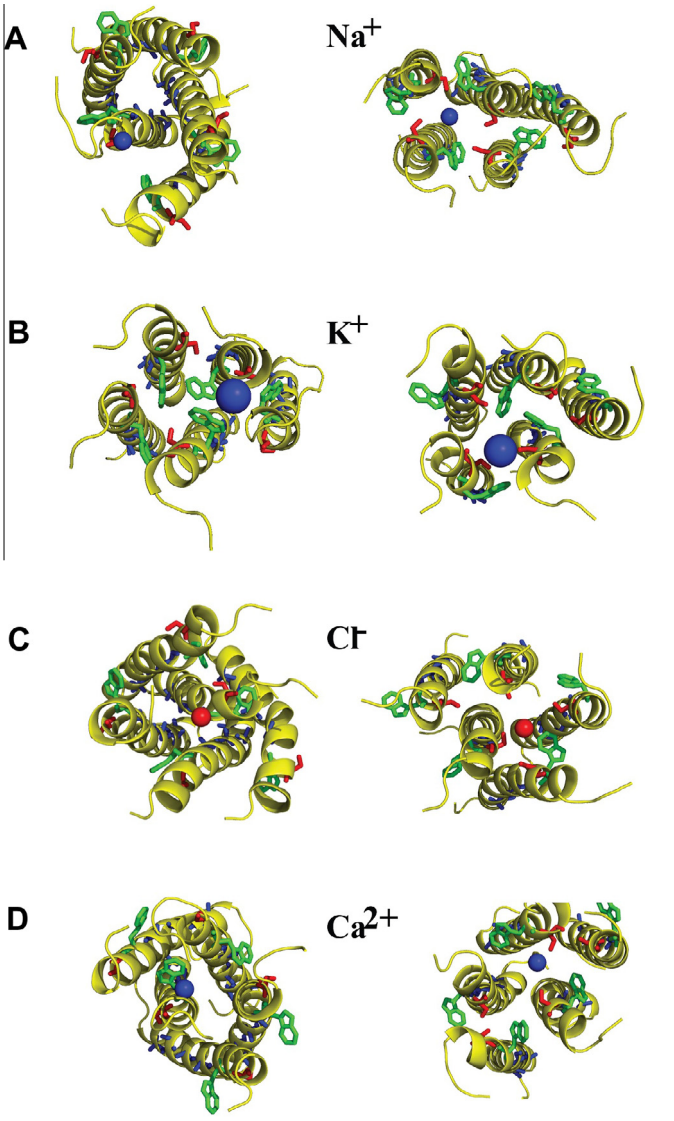

Fig. 4. Lowest-energy bundle structure (left column) and serine-facing-pore structure (right column) of Vpu_{1-32} in the presence of Na^+ (A), K^+ (B), Cl^- (C) and Ca^{2+} (D) after 50 ns MD simulation. The bundles are shown in a top-view from the C to N terminal side. The helix backbone is shown in yellow, alanine residues in blue, serine residues in red and tryptophan residues in green. Cations are shown as a blue, Cl^- as a red sphere. (For interpretation of color in this Figure, the reader is referred to the web version of this article.)

located at the interhelical face and the serines are inside. They could simply rotate or flip outwards to further free ion passage.

Both types of bundle architecture, lowest-energy bundle or serine-facing-pore bundle, turn into more compact structures, eventually a tetramer, in the presence of the restraint single ion. This collapse of the bundle suggests, that Vpu is a kind of 'smooth surface' peptide [29] and suggests further, that for an 'open' structure more ions could be need. The additional ion could be a counter ion. It has been concluded from previous experimental data, that cations and anions should simultaneously pass the bundles [16].

It is consequently suggested that Vpu could conduct ions in various conformations either as a (i) tilted hydrophobic bundle or a (ii) more straight hydrophilic bundle.

There is no unique handedness for the bundles assembled either in the absence [25] or, as reported here, in the presence of ions. Variation in bundle handedness has also been reported for p7 from HCV, which is another viral channel-forming protein [30].

Table 3
Averaged tilt and kink angles, as well as solvent accessible surface area (SAS) of the bundles derived from P-I during a 50 ns MD simulation. Averages of the tilt and kink are taken over the whole trajectory and all TMDs. [1]Δ% of the mean value; [2]M2 helices taken from original structure 3EZH, no restraint ion; [3]M2 helices assembled using the assembly protocol, no restraint ion. The upper line shows data for the lowest-energy bundles, the second line those for serines-facing-pore bundles.

Ion	Tilt [°]	Kink [°]	SAS		
			First ns [nm^2]	Last ns [nm^2]	Δ%[1]
Na^+	21.6 ± 3.5	163.7 ± 3.9	98.2 ± 3.8	82.5 ± 1.6	16.0
	8.9 ± 1.2	167.3 ± 2.6	95.3 ± 2.7	90.8 ± 2.1	4.7
K^+	12.7 ± 5.2	166.1 ± 4.7	91.9 ± 2.6	90.0 ± 1.8	2.1
	15.8 ± 3.5	167.4 ± 2.3	97.8 ± 3.9	86.0 ± 1.9	12.1
Cl^-	27.2 ± 5.9	166.3 ± 5.9	91.6 ± 1.8	85.4 ± 2.1	6.8
	11.2 ± 6.4	164.1 ± 9.9	98.8 ± 3.7	90.5 ± 1.7	8.4
Ca^{2+}	26.7 ± 7.7	163.6 ± 4.9	90.2 ± 3.3	80.8 ± 1.7	10.4
	14.2 ± 5.4	159.3 ± 6.7	105.4 ± 2.7	94.2 ± 1.7	10.6
M2					
Na^+	14.6 ± 9.2	166.5 ± 4.9	68.4 ± 1.5	65.6 ± 1.3	4.1
3EZH[2]	9.5 ± 5.3	162.5 ± 8.3	62.1 ± 2.2	53.3 ± 1.5	14.2
Assembled bundle[3]	9.2 ± 5.1	164.4 ± 5.8	60.4 ± 1.9	58.4 ± 1.2	3.3

4.2. Consistency with experimental data

The formation of a hydrophobic pore would explain the weak experimental ion selectivity reported for Vpu [14–16]. The structural data that indicates the serines and tryptophans point outside [24] are referred to herein as the lowest energy structures or hydrophobic bundles and have average tilt angles at 13°. These data are similar to the data reported in this study primarily for the serine-facing-pore bundles and bundles assembled without ions as previously reported [25]. Thus, the ions may induce a larger tilt in the putative bundle (see previous publications [16] for a discussion on ion-induced 'salting out'). Experiments show that mutating the serines abrogates channel activity, but Vpu can still fulfil, for example, its role as down-modulator of BST-2 [18]. The former findings do not necessarily imply that serines must face the pore. In the light of the hydrophobic pores presented herein, the serines may also be more essential for maintaining structural integrity than supporting ion conductance.

The assembly protocol was also applied to a known pore motif from GLIC [26], which is reported as an open structure of a ligand-gated ion channel. The assembly protocol generates structures that closely represent the experimental motif. Deviations from the experimental structure could result from missing restraints imposed by the remaining TMDs on each GLIC subunit. Interestingly, assembly without ions was less consistent with the crystal structure. Thus, it is worthwhile to speculate how important the ions are during *in vivo* ion channel construction. It is concluded that the Vpu bundles are reliable assemblies based on the good performance of the assembly protocol applied to the GLIC M2s.

Based on computational data from assembling TMDs from Vpu, a potential Vpu bundle could exist as a hydrophobic pore even in the presence of physiologically relevant ions. The presence of ions does not induce formation of a 'hydrophilic' pore. Under the current computational protocol, which does not include the presence of a hydration shell around the ions, the Vpu assembly tends to form a tetramer.

Acknowledgments

WBF thanks the National Science Council of Taiwan (NSC98-2112-M-010-002-MY3) for financial support. We acknowledge the National Center for High-Performance Computing (NCHC), TW for providing computer time and services.

Appendix A. Supplementary data

Supplementary data associated with this article can be found, in the online version, at http://dx.doi.org/10.1016/j.bbrc.2013.11.017.

References

[1] W.B. Fischer, Where is computational bioanalytics?, J Bioanal. Biomed. 4 (2012) 3.
[2] S. Bernèche, B. Roux, Energetics of ion conductance through the K^+ channel, Nature 414 (2001) 73–77.
[3] Y. Zhou, J.H. Morais-Cabral, A. Kaufman, R. MacKinnon, Chemistry of ion coordination and hydration revealed by a K^+ channel-Fab complex at 2.0 Å resolution, Nature 414 (2001) 43–48.
[4] A. Fink, N. Sal-Man, D. Gerber, Y. Shai, Transmembrane domains interactions within the membrane milieu: principles, advances and challenges, Biochim. Biophys. Acta 1818 (2012) 974–983.
[5] W.B. Fischer, Y.-T. Wang, C. Schindler, C.-P. Chen, Mechanism of function of viral channel proteins and implications for drug development, Int. Rev. Cell Mol. Biol. 294 (2012) 259–321.
[6] K. Strebel, T. Klimkait, M.A. Martin, Novel gene of HIV-1, *vpu*, and its 16-kilodalton product, Science 241 (1988) 1221–1223.
[7] E.A. Cohen, E.F. Terwilliger, J.G. Sodroski, W.A. Haseltine, Identification of a protein encoded by the *vpu* gene of HIV-1, Nature 334 (1988) 532–534.
[8] E.F. Terwilliger, E.A. Cohen, Y. Lu, J.G. Sodroski, W.A. Haseltine, Functional role of human immunodeficiency virus type 1 vpu, Proc. Natl. Acad. Sci. USA 86 (1989) 5163–5167.
[9] N. van Damme, D. Goff, C. Katsura, R.L. Jorgensen, R. Mitchell, M.C. Johnson, E.B. Stephens, J. Guatelli, The interferon-induced protein BST-2 restricts HIV-1 release and is downregulated from the cell surface by the viral Vpu protein, Cell Host Microbe 3 (2008) 1–8.
[10] S.J.D. Neil, T. Zang, P.D. Bieniasz, Tetherin inhibits retrovirus release and is antagonized by HIV-1 Vpu, Nature 451 (2008) 425–431.
[11] F.P. Blanchet, J.P. Mitchell, V. Piguet, B-TrCP dependency of HIV-1 Vpu-induced downregulation of CD4 and BST-2/tetherin, Curr. HIV Res. 10 (2012) 307–314.
[12] J.L. Douglas, J.K. Gustin, K. Viswanathan, M. Mansouri, A.V. Moses, K. Früh, The great escape: viral strategies to counter BST-2/tetherin, PLoS Pathog. 6 (2010) e1000913.
[13] U. Schubert, S. Bour, A.V. Ferrer-Montiel, M. Montal, F. Maldarelli, K. Strebel, The two biological activities of human immunodeficiency virus type 1 Vpu protein involve two separable structural domains, J. Virol. 70 (1996) 809–819.
[14] U. Schubert, A.V. Ferrer-Montiel, M. Oblatt-Montal, P. Henklein, K. Strebel, M. Montal, Identification of an ion channel activity of the Vpu transmembrane domain and its involvement in the regulation of virus release from HIV-1-infected cells, FEBS Lett. 398 (1996) 12–18.
[15] G.D. Ewart, T. Sutherland, P.W. Gage, G.B. Cox, The Vpu protein of human immunodeficiency virus type 1 forms cation-selective ion channels, J. Virol. 70 (1996) 7108–7115.
[16] T. Mehnert, A. Routh, P.J. Judge, Y.H. Lam, D. Fischer, A. Watts, W.B. Fischer, Biophysical characterisation of Vpu from HIV-1 suggests a channel-pore dualism, Proteins 70 (2008) 1488–1497.
[17] M.E. Gonzales, L. Carrasco, The human immunodeficiency virus type 1 Vpu protein enhances membrane permeability, Biochemistry 37 (1998) 13710–13719.
[18] S. Bolduan, J. Votteler, V. Lodermeyer, T. Greiner, H. Koppensteiner, M. Schindler, G. Thiel, U. Schubert, Ion channel activity of HIV-1 Vpu is dispensable for counteraction of CD317, Virology 416 (2011) 75–85.
[19] A.L. Grice, I.D. Kerr, M.S.P. Sansom, Ion channels formed by HIV-1 Vpu: a modelling and simulation study, FEBS Lett. 405 (1997) 299–304.
[20] P.B. Moore, Q. Zhong, T. Husslein, M.L. Klein, Simulation of the HIV-1 Vpu transmembrane domain as a pentameric bundle, FEBS Lett. 431 (1998) 143–148.
[21] F. Cordes, A. Kukol, L.R. Forrest, I.T. Arkin, M.S.P. Sansom, W.B. Fischer, The structure of the HIV-1 Vpu ion channel: modelling and simulation studies, Biochim. Biophys. Acta 1512 (2001) 291–298.
[22] F.S. Cordes, A.D. Tustian, M.S. Sansom, A. Watts, W.B. Fischer, Bundles consisting of extended transmembrane segments of Vpu from HIV-1: computer simulations and conductance measurements, Biochemistry 41 (2002) 7359–7365.
[23] A. Kukol, I.T. Arkin, Vpu transmembrane peptide structure obtained by site-specific fourier transform infrared dichroism and global molecular dynamics searching, Biophys. J. 77 (1999) 1594–1601.
[24] S.H. Park, A.A. Mrse, A.A. Nevzorov, M.F. Mesleh, M. Oblatt-Montal, M. Montal, S.J. Opella, Three-dimensional structure of the channel-forming trans-membrane domain of virus protein "u" (Vpu) from HIV-1, J. Mol. Biol. 333 (2003) 409–424.
[25] L.-H. Li, H.-J. Hsu, W.B. Fischer, Assembling vrial channel forming proteins: Vpu from HIV-1, Biopolymers 99 (2013) 517–529.
[26] R.J.C. Hilf, R. Dutzler, Structure of a potentially open state of a proton-activated pentameric ligand-gated ion channel, Nature 457 (2009) 115–119.
[27] J. Krüger, W.B. Fischer, Assembly of viral membrane proteins, J. Chem. Theory Comput. 5 (2009) 2503–2513.
[28] J. Krüger, W.B. Fischer, Exploring the conformational space of Vpu from HIV-1: a versatile and adaptable protein, J. Comput. Chem. 29 (2008) 2416–2424.
[29] T.H.T. Nguyen, N.Z. Rao, W.M. Schroeder, P.B. Moore, Coarse-grained dynamics of tetrameric transmembrane peptide bundles within a lipid bilayer, Chem. Phys. Lipids 163 (2010) 530–537.
[30] D.E. Chandler, F. Penin, K. Schulten, C. Chipot, The p7 protein of hepatitis C virus forms structurally plastic, minimalist ion channels, PLoS Comput. Biol. 8 (2012) e1002702.